A SURVEY OF MEDIUM ENERGY ELECTRONS AT HIGH ALTITUDE BASED ON ISEE-1 DATA

E.J. Daly and C. Tranquille
European Space Agency,
ESTEC
2200AG Noordwijk
The Netherlands

ABSTRACT

The ISEE-1 and ISEE-2 spacecraft explored the outer magnetospheric environment to about 24 earth radii. The MEPI instrument provided data on electron fluxes in the energy range 22-1200 keV. We present results of a survey of a complete data set of isotropic electron fluxes measured by the ISEE-1 spacecraft between November 1977 and September 1979. This analysis provides an overview of the morphology of electrons at these energies, describing the dependence of the electron fluxes on geomagnetic coordinates and local time and showing the probabilities of given particle flux levels being exceeded.

Apart from its general interest, this information is useful in performing engineering evaluations of spacecraft-environmental interactions. ESA is planning or assessing a number of missions which will use highly eccentric earth orbits. Potential problems caused by the particle environments in these orbits include spacecraft charging, deep dielectric charging and electron- and bremsstrahlung-induced background in detectors.

We compare measured particle fluxes with the low-energy part of the electron radiation belt model AE8 and find significant differences. Electron flux enhancements are seen throughout the magnetosphere during solar events.

INTRODUCTION

Several future ESA programs will make use of highly-eccentric synchronous orbits for space-based astronomy. Typical of this type of orbit are the 24-hour orbit with apogee around 71000 km and the 48-hour orbit with apogee around 120000km. Inclinations in the range 7° - 60° are possible. For astronomy, these orbits provide extended observing time, reduced interference from the near-earth environment and good ground-station coverage. Similar orbits are under consideration for high-latitude communications satellites and navigation satellites. US and Soviet programs also make use of such orbits. Clearly these orbits will pass through the 'trapped radiation belts', through parts of the magnetosphere well known for electrostatic charging problems, and will also be exposed to solar particle fluxes.

The work outlined in this paper was prompted by the need to evaluate environmental interactions at the high altitudes (and therefore high geomagnetic L-values) reached by such orbits and by the lack of data from these regions in a useable form. Most data relating to charging and energetic particle interactions in Earth orbit concentrate on lower altitudes. The geostationary orbit is particularly well covered. The AE8 model for the energetic electron environment only gives data out to L = 11 R_e.

Environmental-interaction concerns include electrostatic charging of surfaces [Frezet et al., 1989], deep-dielectric charging, and interference with the detectors of the payload. Detectors flown on astronomy satellites are very sensitive and are susceptible to background noise caused by the ambient particle environment. Primary or secondary particles can cause this background. X-ray detector systems using grazing-incidence mirror systems are also potentially exposed to particles scattering through the mirrors.

Recently, much attention has been given to the correlation between relativistic electrons (of several MeV in energy) at 6.6 R_e [Baker et al., 1989] and their effect on the operation of geostationary spacecraft [Baker et al., 1987]. The AE8 model is poorly suited to evaluate these effects for higher altitude eccentric orbits. For such an evaluation, extremes of fluxes are needed rather than average values.

The AE8 model provides average omnidirectional electron fluxes ranging in energy from 40 keV to 7 MeV. Fluxes at the high energy limit are mainly extrapolated from lower energy data. AE8 extends out to 11 R_e. Extrapolation from lower altitude data is often used to provide values at this outer radial limit. The AE8 model is a static model and takes no account of the many dynamic processes which are known to occur in the magnetosphere over short time scales. There is also no dependence on geomagnetic activity or on the interplanetary magnetic field and solar wind conditions.

A local time model was built into the AE4 electron flux model and has been adapted by us for use with AE8. The local time variation of the logarithm of the flux is modelled as sinusoidal, characterised by an amplitude and a phase term, both varying as functions of energy and L.

Confidence levels for exceeding specified fluxes can also be defined by parameterising the Gaussian distribution of the logarithm of the fluxes used to define the AE4 model.

To date, no quantitative synoptic analysis has been made for charged particles outside of the Van Allen belts, and only transitions through isolated magnetospheric structures have been investigated. The standard models of the trapping region also require a new analysis, given that they are constructed from measurements made in the sixties and early seventies, and have not yet been updated to include more contemporary data sets.

The data on electron fluxes from by the Medium Energy Particle Instrument (MEPI) flown on the ISEE-1 satellite were selected for study. We compare the MEPI measurements made in the Van Allen belts with those derived from the AE8 model [Vette, 1989]. We also obtain confidence levels that given flux values will not be exceeded, as a function of L-value and electron energy.

THE ISEE-1 ORBIT AND INSTRUMENTATION

ISEE-1 was launched on October 22, 1977, as one of three satellites designed to investigate the inter-relationship between solar and geomagnetic phenomena [Ogilvie et al., 1978]. The initial orbit of ISEE-1 had an apogee of 22.6 R_e, a perigee of 270 km, a period of 57.2 hours and an equatorial inclination of 28.3°. Throughout the year, the orientation of the apogee of this orbit with respect to the sun-earth line rotates so that all local times are sampled. As a consequence, most magnetospheric features were visited. At launch, the orbit apogee was almost at noon local time. The daughter spacecraft, ISEE-2, had almost identical orbital parameters. The separation of the two satellites could be accurately controlled to make dual spacecraft measurements, with high spatial resolution. All ISEE spacecraft were equipped with a variety of instruments to measure particle, magnetic field, electric field and solar wind properties. The ISEE-1 satellite also provided data for the multi-spacecraft International Magnetospheric Study (IMS) [Ogilvie, 1984].

The Medium Energy Particles Instrument [Williams et al., 1978] was designed to measure electrons and ions with high temporal, angular and energy resolution. The hardware development was made by the Space Environment Laboratory at NOAA (USA), the Max-Planck Institute for Aeronomy (FRG) and the University of Kiel (FRG).

The energy range of the detector is 22.5 to 1200 KeV for electrons. This range is divided into eight logarithmically equidistant channels, as detailed in Table 1. Data were also acquired at high bit-rate but these are converted to low bit-rate for inclusion into the data set we use. In addition, the directional data provided by scanning and spinning are are used to produce omni-directional fluxes with a time resolution of approximately 5 minutes.

Channel Number	Energy Range (keV)
E1	22.5 - 39
E2	39 - 75
E3	75 - 120
E4	120 - 189
E5	189 - 302
E6	302 - 477
E7	477 - 756
E8	756 - 1200

Table 1: MEPI Electron Energy Channels

MEPI measurements were made by ISEE-1 from launch to September 11, 1979, after which a failure in the power supply of the experiment resulted in the loss of the instrument. A total of 281 orbits were completed during the 670 days of the instrument's operation, starting 1.5 years after solar minimum and therefore covering the 'run-up' to solar maximum.

The data were provided to us by D.J. Williams and D.G. Mitchell of the Applied Physics Laboratory, Johns Hopkins University.

A similar electron experiment was flown by the ISEE-2 satellite, although with inferior energy and angular resolution. This experiment continued to make measurements right up until contact with the daughter satellite was lost, some ten years after launch (September 26, 1987).

ORBIT COVERAGE

The suitability of the ISEE-1 orbit for investigating the radiation environment for highly eccentric orbits is shown in Figure 1.

Each electron flux measurement made by MEPI is recorded with ancillary information, including UT and position in GSE coordinates. Mapping to geomagnetic B-L coordinates requires a series of transformations, together with the use of a magnetic field model. In our analysis reported here we have used an internal model of the field. This is known to provide poor information at high altitudes where external current systems strongly affect the field. However, it is used solely as an organisational aid for comparison with models and other satellite data, which also use an internal model. In future work, we hope to employ an external model such as that described by Tsyganenko [1989]. The model we use is the International Geomagnetic Reference Field (IGRF) for 1980 [Peddie, 1982]. In geomagnetic B, L coordinates there is no information about local time, therefore this is also computed.

All valid MEPI measurements were mapped into geomagnetic B-L space and the total number of data points available in each cell found. This is shown in Figure 1. The geomagnetic equator is drawn as a continuous line in the figure.

Data coverage is best above 12 R_e and close to the equator. At lower altitudes, the coverage becomes very sparse, due to the relatively quick transition through perigee, when compared to the longer periods spent close to apogee. Nevertheless, down to about 4 R_e, the coverage is acceptable when the spacecraft is not far from the magnetic equator. Above 12 R_e, the coverage is excellent, albeit limited in terms of B. If the equatorial pitch angle distribution of the electrons is known, it is possible to derive fluxes at higher B values (higher latitudes) [Garcia and Spjeldvik, 1985].

The baseline orbits of the forthcoming XMM (X-ray), ISO (infra-red) and FIRST (far infra-red) missions are projected into the geomagnetic coordinate system to illustrate the suitability of the ISEE-1 orbit for the present study. The XMM orbit is a 24 hour orbit of 60° inclination, and apogee height of ~ 71000 km. ISO has a similar orbit, but with a low inclination of 5°. The period of the FIRST orbit is 48 hours, with apogee at ~ 120000 km and again a 5° inclination. Both the ISO and FIRST orbits are totally enclosed by the ISEE-1 orbit, as is the high inclination XMM orbit below about 20 R_e.

ELECTRON FLUX PROFILES

Figures 2-4 show examples of thirty-day plots of electron fluxes in 4 of the eight MEPI energy channels. Flux increases seen in the electron count rates are clearly identifiable with the radiation belts, with energetic populations in the tail and with solar flare events. When the apogee is in the upstream region, the electron flux profiles are very clean, with the belt transitions easily distinguishable. However, when the apogee is situated in the magnetotail, the belt transitions are somewhat difficult to isolate due to the many flux enhancements seen on short timescales outside the trapping region. This is especially true at the lower energies, where high fluxes are maintained almost constantly between Van Allen belt passes.

Superimposed on the electron flux profiles, are examples of solar electron events which are easily recognisable by significant (two orders of magnitude, in the lowest energy channel) flux enhancements seen simultaneously across the complete energy range of the instrument. Associated with these events are solar flare protons and alpha particles. A table of solar proton events has been compiled by Goswami et al. [1988]. Using this table, solar flare events have been independently identified (the arrow at the bottom of the first panel) to confirm the association of the long term electron flux enhancements with flare activity on the sun in the majority of cases. Some electron events have no solar proton counterpart. Inspection of plots of IMP-7 and -8 data [Solar-Geophysical Data Comprehensive Reports] reveals a similarity between the energetic proton time behaviour and the time behaviour of the ISEE-1 MEPI electron fluxes, although this is not always the case.

Solar flares and shock fronts can also be detected from solar wind and magnetic field measurements in the interplanetary medium. A distinct signature is the sudden increase in the interplanetary solar wind velocity, V_{sw}, to well above the nominal value of 400 km/s. The third panel of the figures shows this particular solar wind behaviour very clearly for the relevant events. The solar wind velocity data were obtained from the on-line database (OMNI) supported by NSSDC. They are compiled from measurements provided by IMP-6 , -7 and -8.

PROCESSING RESULTS

The MEPI data were used to define electron fluxes in each of the 8 energy channels for the parts of B-L space covered by ISEE-1. Average fluxes were computed for B, L bins and these are shown in Figure 5 (channel 2) and Figure 6 (channel 5).

When compared to predictions from the AE8 electron model, we find that fluxes are somewhat lower than predicted. Also clear from Figures 5 and 6 is the severe truncation of AE8 fluxes at around 11 R_e.

Within a number of L-bands, a distribution of electron fluxes within each channel was created. These are shown in Figure 7 for $6 < L < 7$, $9 < L < 10$ and $12 < L < 13$ in the form of plots of the percentage of data having fluxes below the value on the x-axis. These indicate the great variability of possible fluxes at given L-values. This kind of processing has been performed in the past for Geostationary orbit [Baker et al., 1981] and for the SCATHA satellite [Mullen and Gussenhoven, 1983]. Our results compare favourably with similar plots given by Mullen and Gussenhoven [1983] in the SCATHA Environmental Atlas. These plots show how the fluxes in the high energy channels remain close to the backround level for most of the time at high L-values (7(c)) while displaying a considerable spread at low L (7(a)).

Fluxes were scatter-plotted against local time for various 1 R_e-wide L bins. These are shown in Figures 8-10 for the energy channels 22.5-39 keV, 120-189 keV and 302-477 keV respectively. Distributions of particle fluxes were produced within 3-hour wide local-time bins, from which the mean (50% probability) and worst-case (95%) values of the logarithm of the flux can be derived as a functions of L and local time. These are superimposed in Figures 8-10 as solid histograms. The limits of the data-set, in terms of the number of data points, becomes somewhat apparent when this is done since the number of data points making up the >95% class are small. Clearly, the 10-year ISEE-2 data set would be very useful for performing this kind of analysis. It should be noted that the plots include fluxes from solar events and so are not clean pictures of magnetospheric electrons. Nevertheless, the changing shape of the distribution of fluxes in local time reflects the electron morphology of the magnetosphere.

Figure 8 shows that, for low energies at low L, the spread of fluxes is relatively small around noon local time, with a peaking in fluxes towards the dawn quadrant. Fluxes are high at all local times although the occasional low-flux data points occur preferentially on the night side. As L increases, this pattern changes so that fluxes are low around noon, beyond the magnetopause, and are higher in the anti-sunward plasma sheet region. A bias in high flux locations towards the dawn quadrant remains. At high L there is a considerable scatter in flux levels, reflecting the dynamicism of the plasma sheet population. The 50% and 95% levels follow this changing behaviour.

The 120-189 keV electron fluxes shown in figure 9 exhibit basically the same characteristics. High fluxes at high L values are encountered principally in the dawn quadrant although fluxes are generally low. Figure 10 (302-477 keV) shows low fluxes at $L \sim 12$ but a similar behaviour to the lower energy channels at lower L.

The MEPI measurements were made in the period leading up to maximum activity of solar cycle 21, which in terms of average solar flare proton flux, was less severe than the preceding two cycles [Goswami et al., 1988]. Indeed, the current maximum in solar activity has already produced several flares of greater intensity than seen at any time during cycle 21.

Solar electron event flux measurements made by ISEE-1 outside of the Van Allen belts do not seem to have any spatial variation, and their profiles are essentially determined by the temporal evolution of the particles as they pass the earth. The severity and duration of the flares are variable, but some have flux increases two or three orders of magnitude above the normal background level. Such enhancements, although only lasting for a few days, can have a very detrimental effect on sensitive detectors and electronics.

CONCLUSIONS AND FUTURE WORK

Electron flux data from the complete energy range of the ISEE-1 MEPI instrument, covering the lifetime of the instrument have been analysed to provide a preliminary basis for evaluation of the energetic electron environment of highly eccentric orbits. The data have been analysed and the general morphology of energetic electrons with respect to geomagnetic coordinates and local time has been established. "Worst-case" data on the electron environment have been produced which should prove valuable for evaluating background and other effects for future missions in these regions. Related to this are the flux-probability plots produced. The local time scatter-plots reveal the morphology of electrons in the magnetosphere and their variability in the various regions. A report containing a more complete set of plots than given here is in preparation [Tranquille et al., 1990].

It is found that in regions of space where there was overlap with existing environment models, these models appear to be pessimistic for this period. In regions beyond the model limits, where modelling normally assumes zero fluxes, there were still non-negligible electron fluxes.

Partial overlap between the data on the particle-induced background of the Cos-B X-ray instrument and the ISEE particle data allowed us to look at their correlation. It is found that "flaring" of the Cos-B background coincides with solar or magnetospheric events observed by ISEE-1 in the majority of cases [Tranquille et al., 1990]. However, this correlation is less than perfect, probably because of the different locations of the two spacecraft in the magnetosphere which, as has been pointed out,is highly dynamic.

There are many possible ways in which this work could be usefully extended. As pointed out above, the ISEE-1 energetic electron data only covers a period of approximately 2 years preceding solar maximum. The equivalent instrument flown by ISEE-2, although measuring electrons of slightly lower maximum energy and at lower energy and angular resolution, collected data over a period from launch to well over ten years later, covering almost a complete solar cycle. Analysis of these data would firstly increase the statistical value of the present study, as well as providing an insight into the solar cycle dependence of the terrestrial electron environment.

A more detailed correlation between flux measurements and solar wind and geomagnetic parameters could also be performed, and, as pointed out above, the Tsyganenko external field model could be employed, incorporating activity and diurnal effects. Equatorial pitch angle distributions could also be used to derive fluxes at higher B values (and therefore higher magnetic latitudes), giving flux information which would be directly applicable to more inclined eccentric orbits.

Data from other spacecraft also exist, for which a similar analysis can be performed. Geostationary data sets from the Los Alamos National Laboratory and from NOAA could be used. These sets overlap ISEE-1 and -2 data in time.

The advantage of using data from other spacecraft is twofold: firstly, it allows flux measurements to be inter-compared, hence enhancing the confidence of the analysis; secondly, it complements the overall data coverage (such as the relatively poor sampling of ISEE-1 at lower altitudes).

Finally, an alternative model to the AE8 model could be constructed using data from the ISEE satellites, and any other suitable sources, with the functionality required for the evaluation of interactions at high altitude. Work to this effect has already been initiated. Following the impending launch of the Combined Release Radiation Effects Satellite (CRRES) [Gussenhoven et al., 1985], an extensive modelling activity will be undertaken.

ACKNOWLEDGEMENTS

We are grateful to D.J. Williams and D.G. Mitchell of the Applied Physics Laboratory, Johns Hopkins University, for providing the MEPI data and for their continued help during processing. We also thank NSSDC for data on solar wind speed and geomagnetic indices from their on-line OMNI database.

REFERENCES

Baker, D.N., R.D. Belian, P.R. Higbie, R.W. Klebesadel and J.B. Blake, Hostile Energetic Particle Radiation Environments in the Earth's Outer Magnetosphere, in *The Aerospace Environment at High Altitudes and its Implications for Spacecraft Charging and Communications, AGARD Conference Proceedings No. 406*, 1987.

Baker, D.N., J.B. Blake, L.B. Callis, R.D. Belian and T.E. Cayton, Relativistic electrons near geostationary orbit: evidence for internal magnetospheric acceleration, *Geophys. Res. Lett., 16*, 559, 1989.

Baker, D.N., P.R. Higbie, R.D. Belian, W.P. Aiello, E.W. Hones, Jr, E.R. Tech, M.F. Halbig, J.B. Payne, R. Robinson, S. Kedge, The Los Alamos Geostationary Orbit Synoptic Data Set, A Compilation of Energetic Particle Data, *LA-8843*, 1981.

Frezet, M., E.J. Daly, J.P Granger and J. Hamelin, Assessment of Electrostatic Charging of Satellites in the Geostationary Environment, *ESA Journal, 13*, 89, 1989.

Garcia, H.A. and W.N. Spjeldvik, Anisotropy characteristics of geomagnetically trapped ions, *J. Geophys. Res., 90*, 347, 1985.

Goswami, J.N., R.E. McGuire, R.C. Reedy, D. Lal and R. Jha, Solar flare protons and alpha particles during the last three solar cycles, *J. Geophys. Res., 93*, 7195, 1988.

Gussenhoven, M.S., E.G. Mullen, R.C. Filz, D.H. Brautigam and F.A. Hauser, New low altitude dose measurements, *IEEE Trans. Nucl. Sci., NS-34*, 676, 1987.

Gussenhoven, M.S., R.C. Filz, K.A. Lynch, E.G. Mullen and F.A. Hauser, Space radiation dosimeter SSJ' for the block 5D/flight 7 DMSP satellite: calibration and data presentation, *AFGL-TR-86-0065*, Air Force Geophysics Laboratory, Hanscom AFB, Ma., 1986. **ADA172178**

Gussenhoven, M.S., Mullen, E.G. and Sagalyn, R.C., CRRES/SPACERAD Experiment descriptions, *AFGL-TR-85-0017*, Air Force Geophysics Laboratory, Hanscom AFB, Ma., January 1985. **ADA160504**

Lyons, R.L. and Williams, D.J., *Quantitative Aspects of Magnetospheric Physics*, D. Reidel Publ. Co., Dordrecht and Boston, 1984.

McIlwain, C.E., Coordinates for mapping the distribution of geomagnetically trapped particles, *J. Geophys. Res., 66*, 3681, 1961.

Mullen, E.G. and M.S. Gussenhoven, SCATHA Environment Atlas, *AFGL-TR-83-0002*, 1983. **ADA131456**

Ogilvie, K.W., Some contributions to knowledge of the magnetospheric plasma by ISEE-1 investigators, in Achievements of the international magnetospheric study (IMS), *ESA SP-217*, 25, 1978.

Ogilvie, K.W., A. Durney and T. von Rosenvinge, Description of experimental investigations and instruments for the ISEE spacecraft, *IEEE Trans. Geosci. Electron., GE-16*, 151, 1978.

Peddie, N.W., International geomagnetic reference field: the third generation, *J. Geomag. Geoelectr., 34*, 309, 1982.

Schulz, M., Earth's radiation belts, *Rev. Geophys. Space Phys., 93*, 77, 1982.

Share, G.H., J.D. Kurfess, K.W. Marlow and D.C. Messina, Geomagnetic origin for transient particle events from nuclear reactor-powered satellites, *Science, 244*, 444, 1989.

Singley, G.W. and J.I. Vette, The AE-4 model of the outer radiation zone electron environment, *NSSDC/WDC-A-R&S 72-06*, National Space Science Data Center, 1972.

Solar Geophysical Data Comprehensive Reports, published monthly by NOAA, U.S. Dept. of Commerce.

Teague, M.J. and J.I. Vette, The inner zone electron model AE-5, *NSSDC/WDC-A-R&S 72-10*, National Space Science Data Center, 1972.

Teague, M.J. and J.I. Vette, AE 6: a model environment of trapped electrons for solar maximum, *NSSDC/WDC-A-R&S 76-04*, National Space Science Data Center, 1976.

Tranquille, C. and E.J. Daly, The radiation environment for earth-orbiting astronomical satellites, submitted to *J. British Inter. Soc.*, 1989.

Tranquille, C., E.J. Daly, D.G. Mitchell and D.J. Williams, A Synoptic Survey of Magnetospheric Energetic Electron Fluxes as Measured by the ISEE-1 Spacecraft, ESTEC Internal Report in preparation, 1990.

Tsyganenko, N.A., A magnetospheric magnetic field model with a warped tail current sheet, *Planet. Space Sci., 37*, 5, 1989.

Vette, J.I., Trapped radiation models, in *Development of Improved Models of the Earth's Radiation Environment, Technical Note 1 (Chapter 4), ESA Contract 8011/88*, IASB, 1989.

Williams, D.J., E. Keppler, T.A. Fritz, B. Wilken and G. Wibberenz, The ISEE 1 and 2 medium energy particles experiment, *IEEE Trans. Geosci. Electron., GE-16*, 270, 1978.

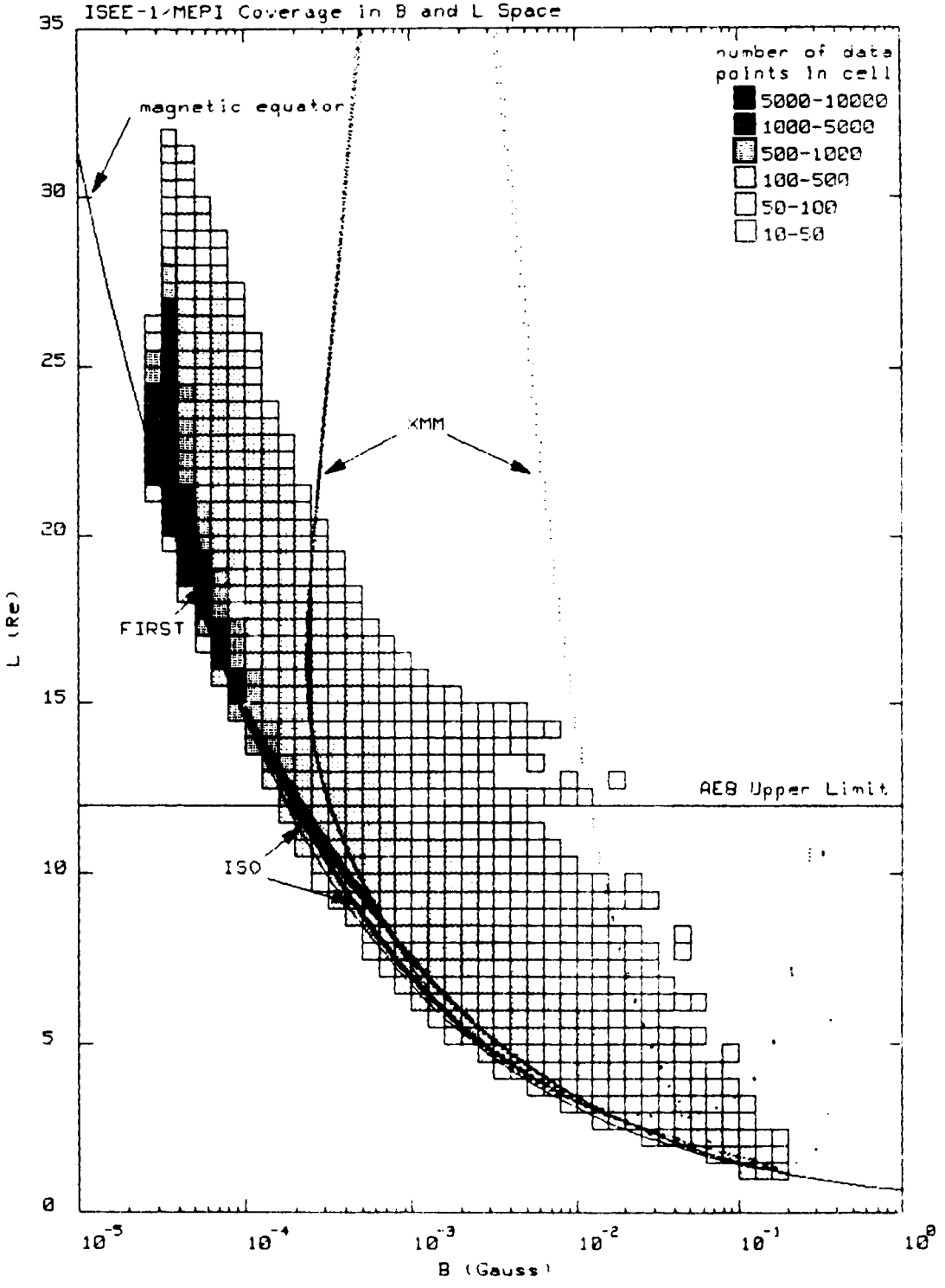

Figure 1: Orbit coverage of the ISEE-1 satellite in terms of geomagnetic coordinates. Gray scale coded cells in B, L space indicate the number of data points available. The geomagnetic equator is shown for reference, as are the $B - L$ traces of the orbits of the future XMM, FIRST and ISO missions.

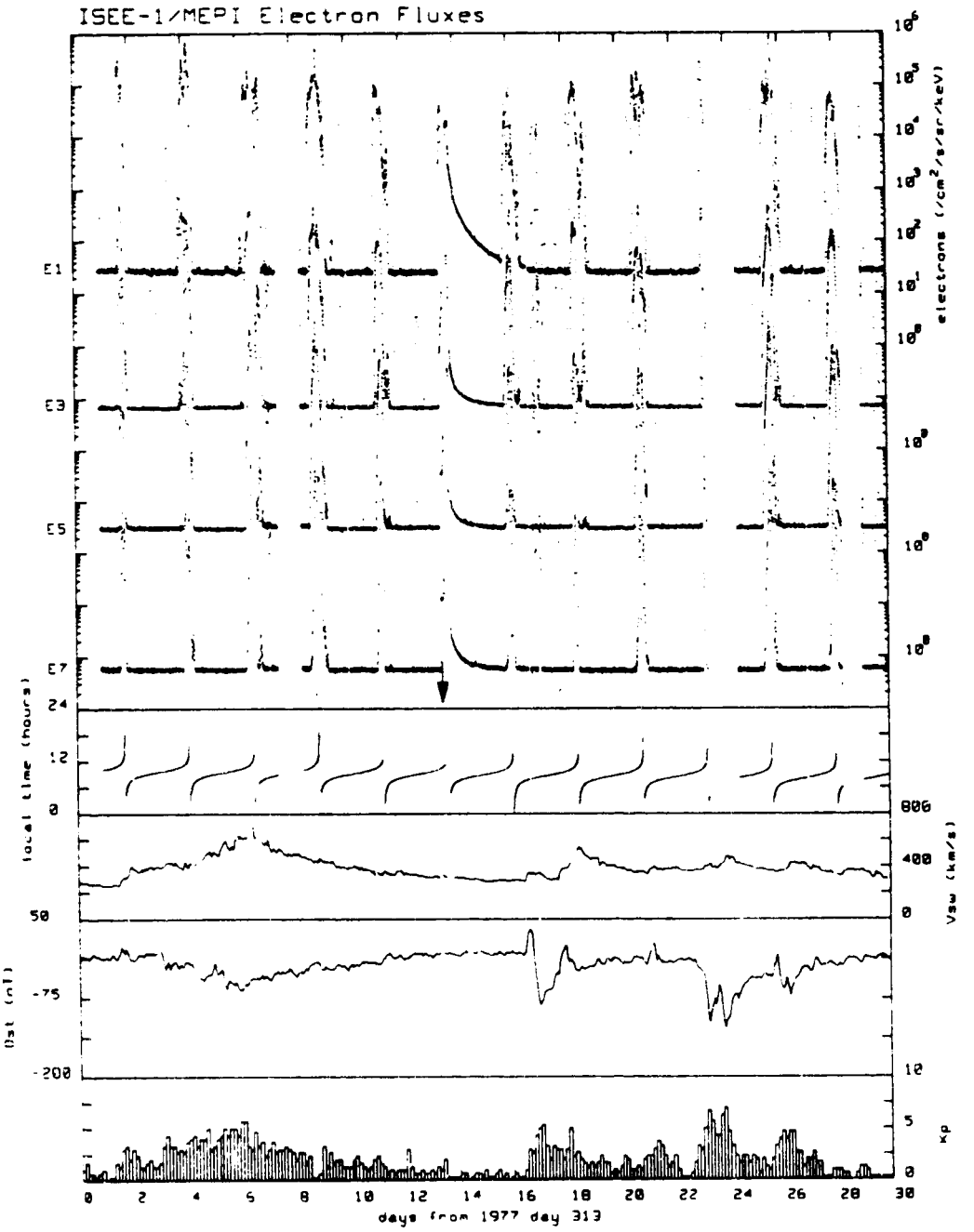

Figure 2: Thirty-day plot of MEPI data from 4 channels, showing quiet conditions (upper panel). The other panels show, from the top, satellite local time, solar wind speed, the D_{st} index and the K, index. Arrows indicate the start of a solar proton event observed by IMP.

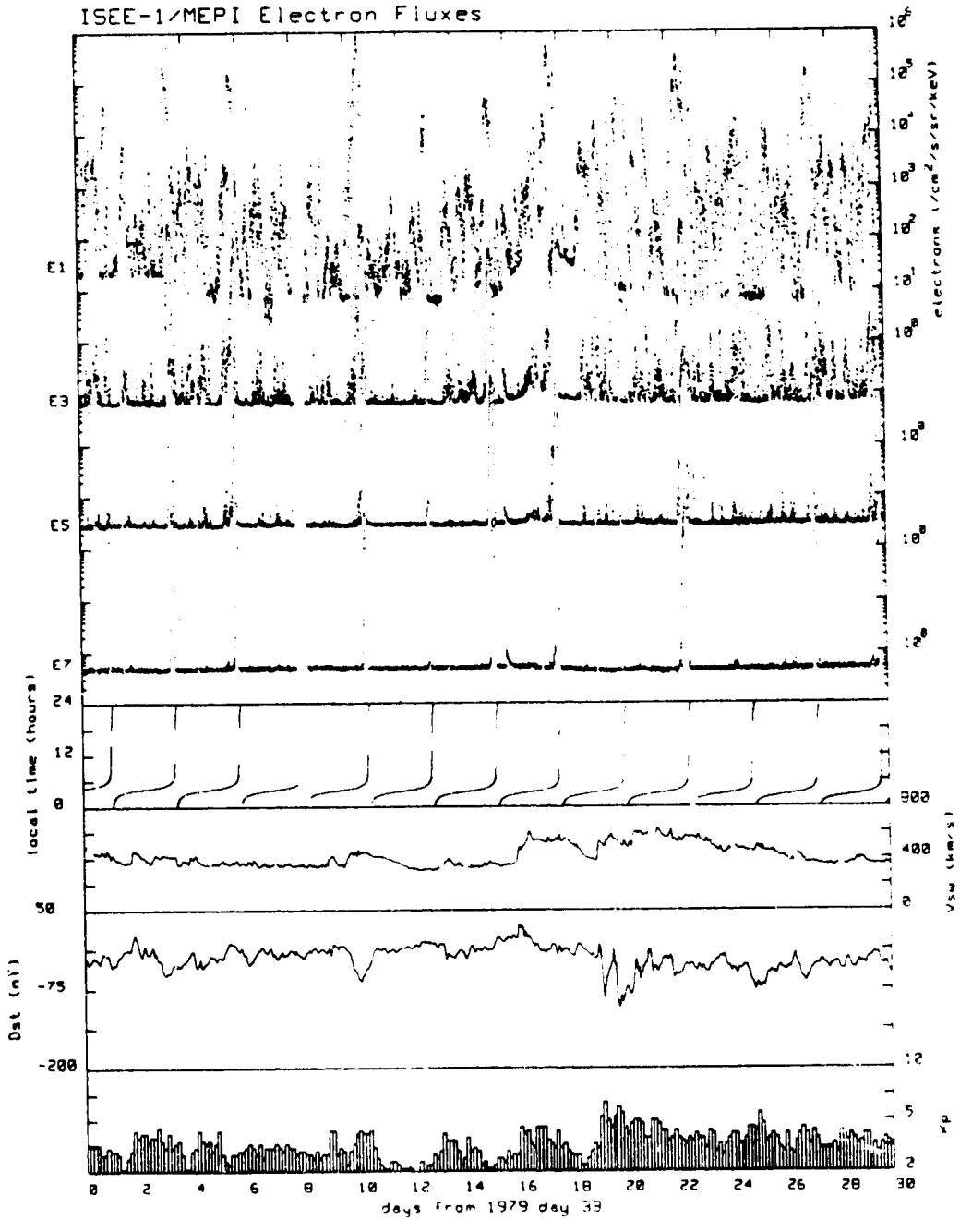

Figure 3: As figure 2 but showing disturbed conditions.

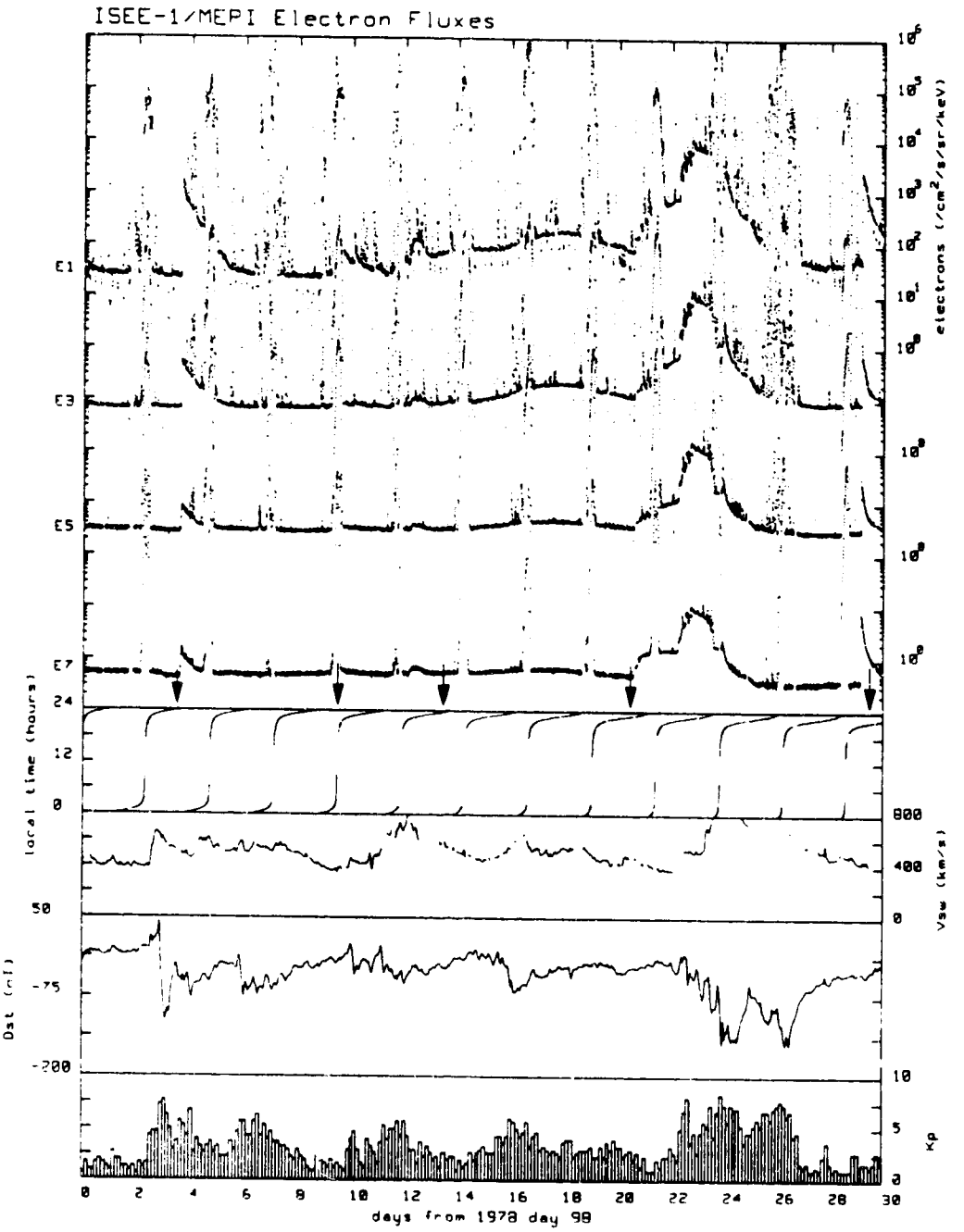

Figure 4: As the previous two figures but showing a solar event.

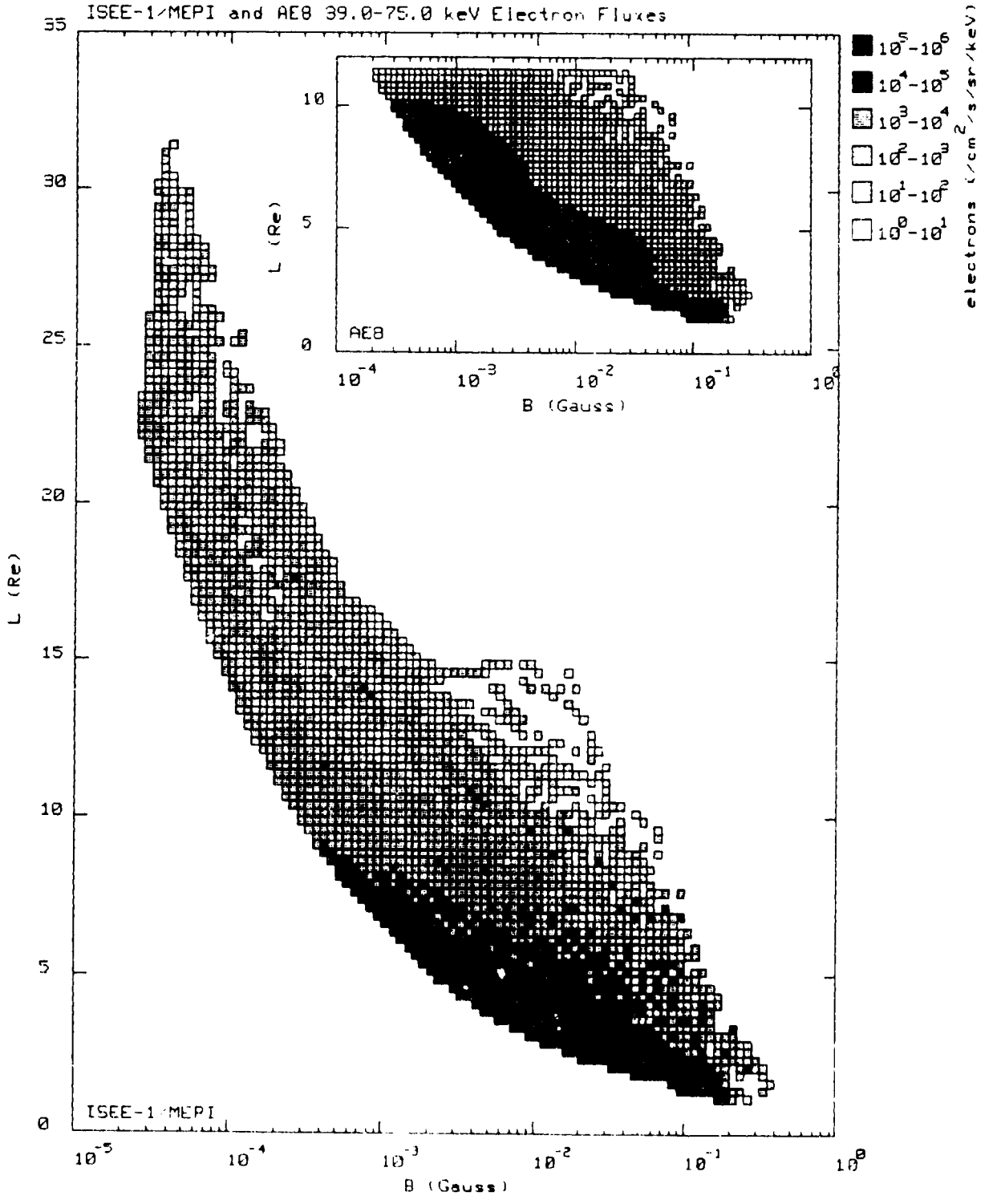

Figure 5: Differential electron fluxes for MEPI channel 2 (39 - 75 keV) are presented as a function of geomagnetic coordinates, B and L, sampled by the ISEE-1 orbit. The inset shows the predictions of the AE8 model for the same energy range.

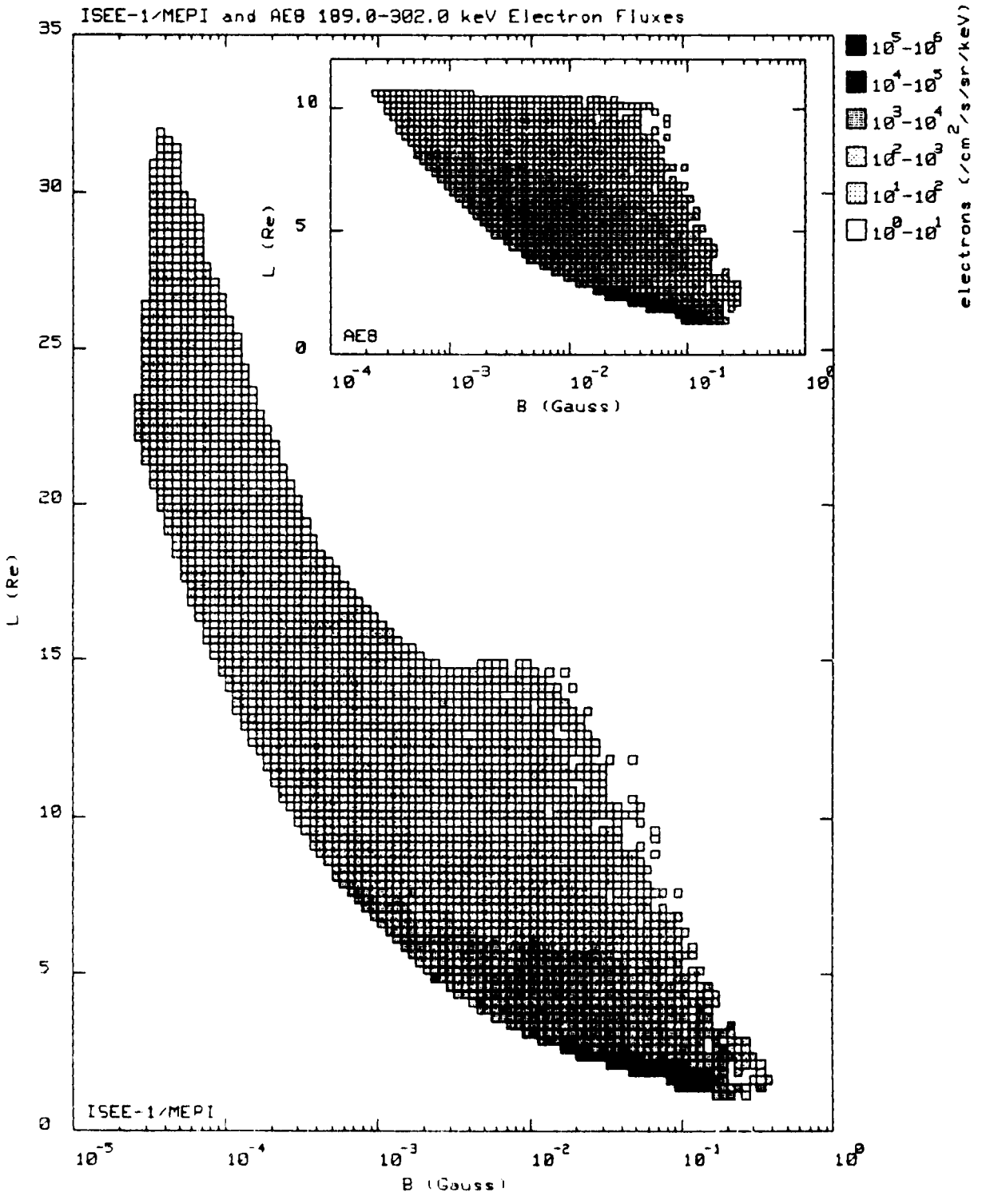

Figure 6: As figure 5 but showing data from channel 5 (189 - 302 keV).

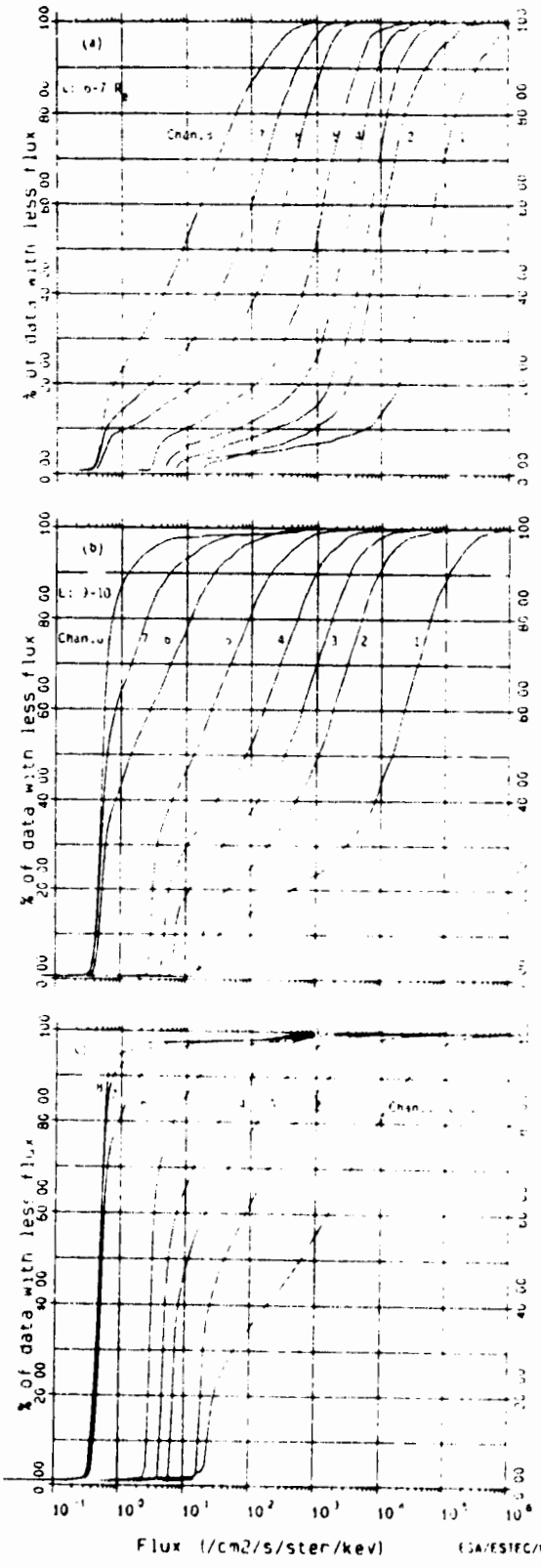

(a)
$6 < L < 7$

(b)
$9 < L < 10$

(c)
$12 < L < 13$

Figure 7: Flux probabilities: plots of the probability of fluxes being below given values, for all 8 MEPI channel energy ranges, for 3 ranges of L: (a) $6 < L < 7$; (b) $9 < L < 10$; (c) $12 < L < 13$.

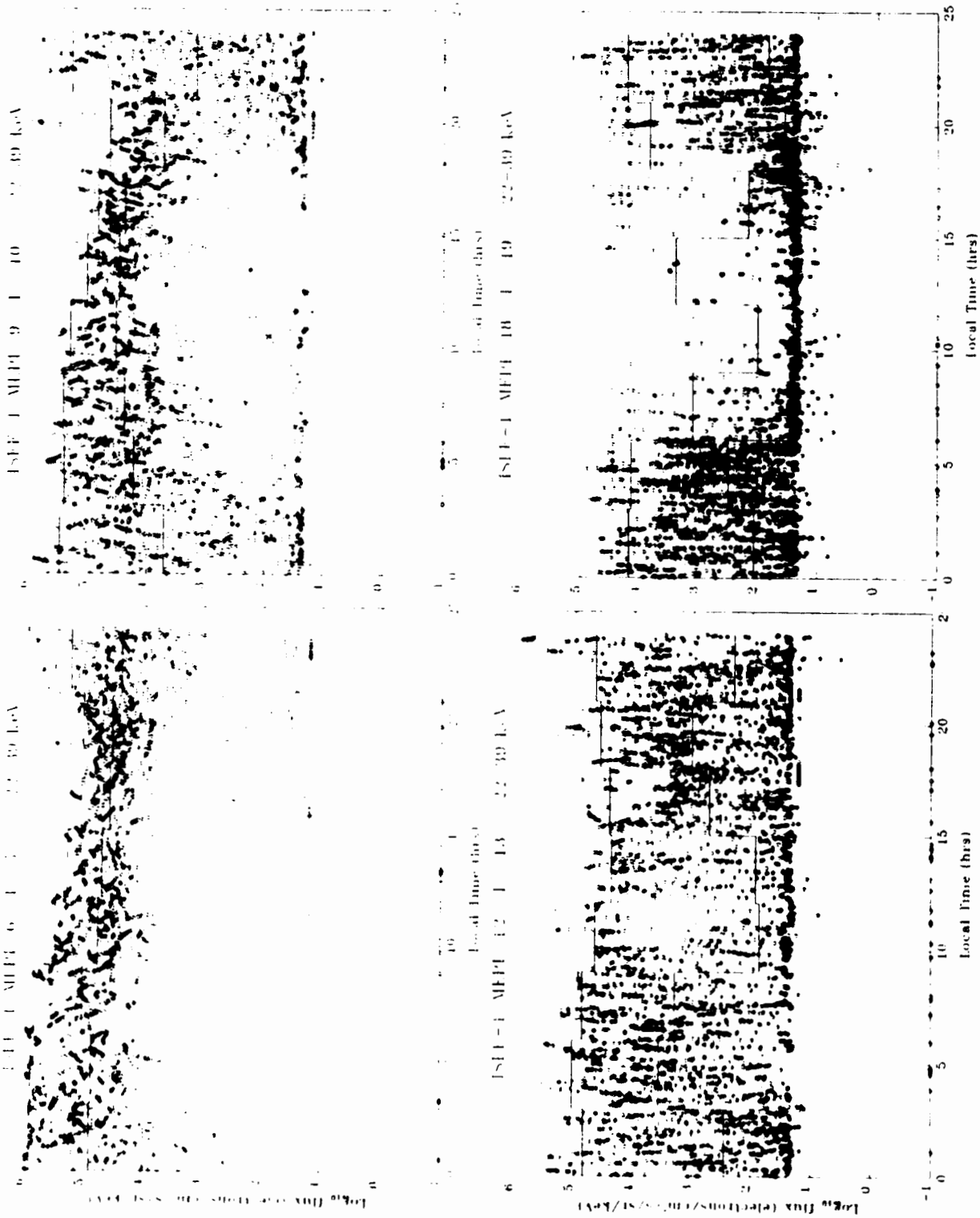

Figure 8: Scatter plots of Log_{10} 22.5-39 keV electron fluxes as functions of local time. Also shown are the mean (50 percentile) and worst-case (95 percentile) log-fluxes. Each plot shows a different L range. The transition from radiation-belt to plasma sheet morphology is clear.

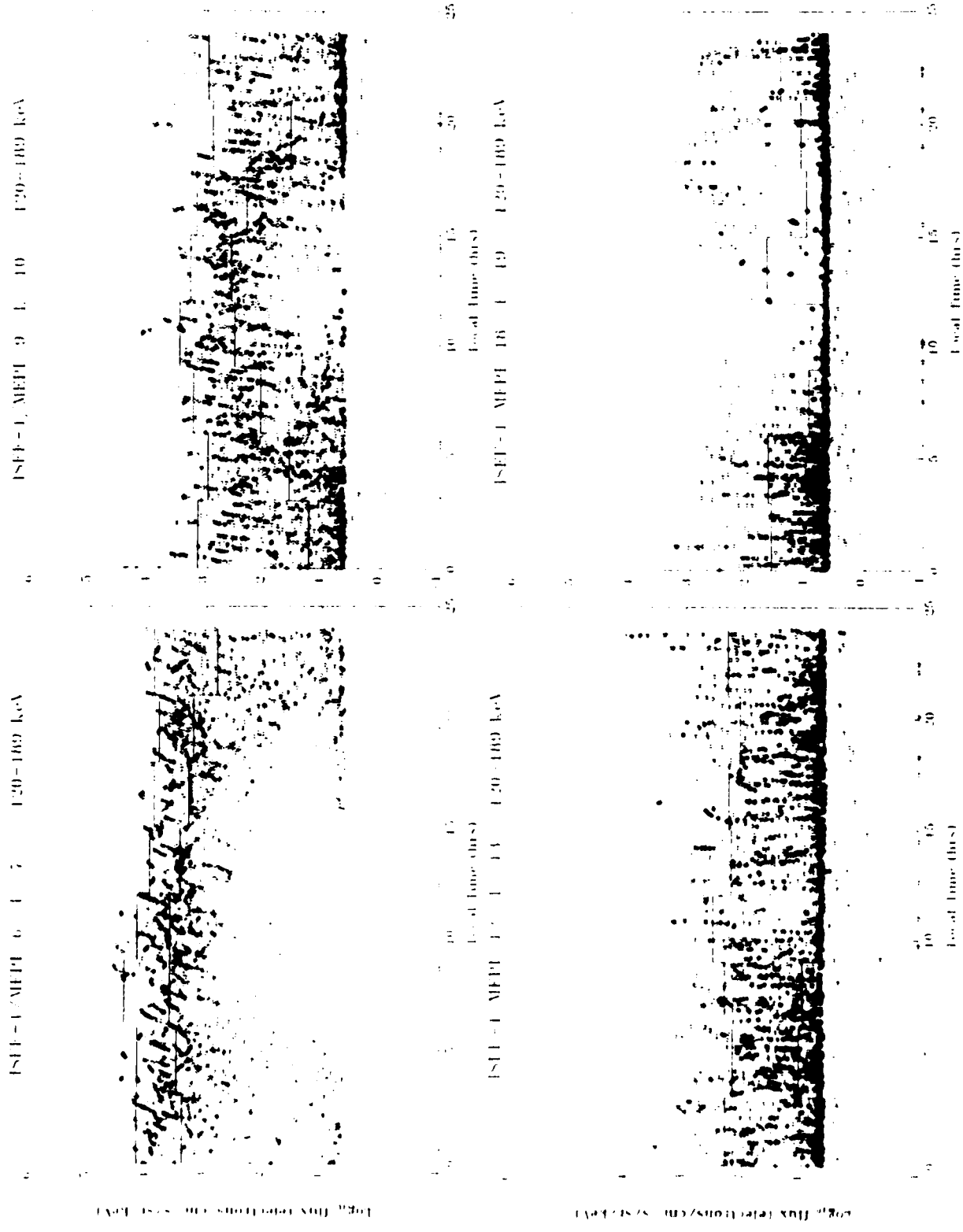

Figure 9: As figure 8 but for MEPI channel 4 (120-189 keV).

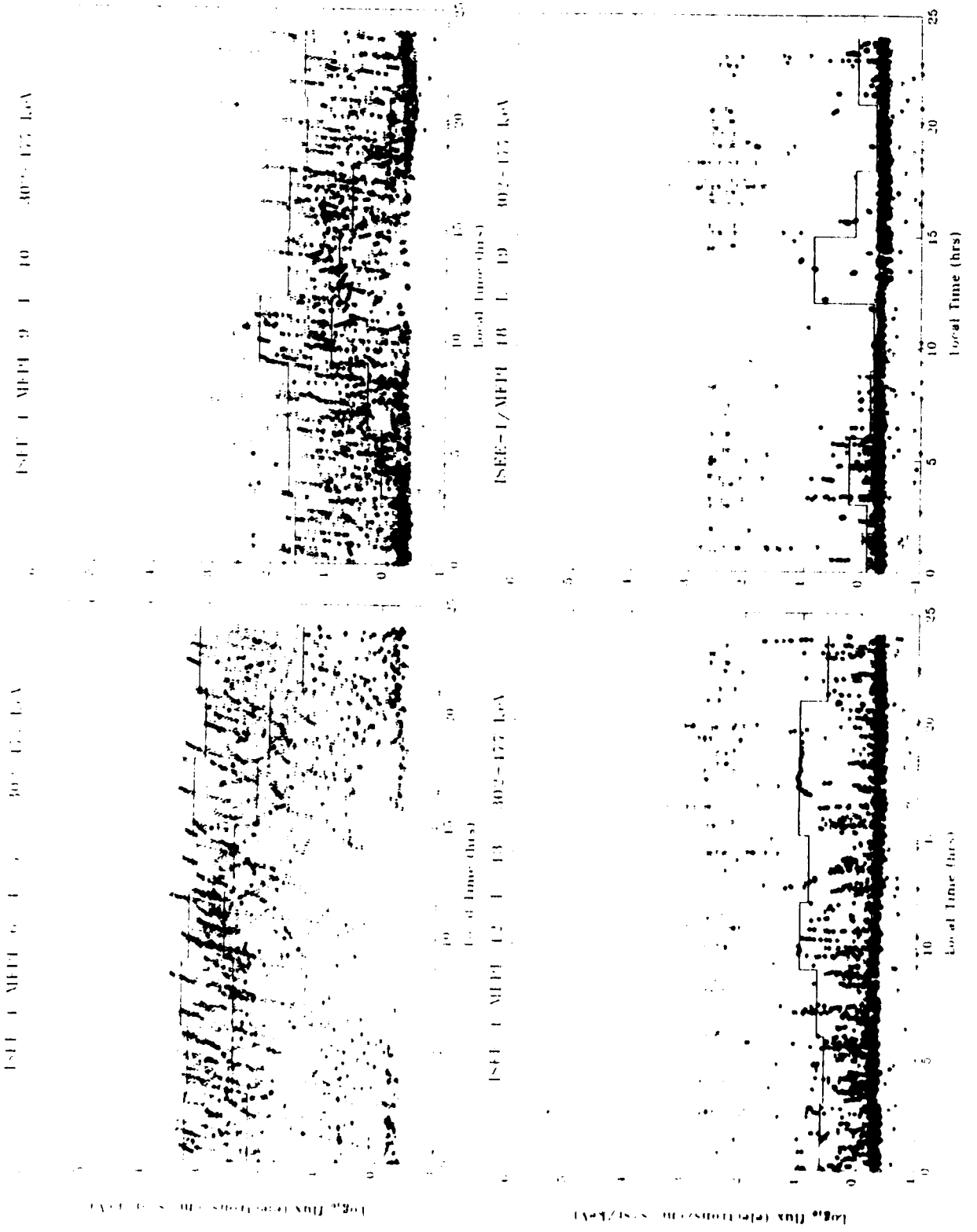

Figure 10. As figure 9 but for MEPI channel 6 (302-477 keV).